

# RADAR-INVISIBILITY ON AXIS OF ROTATIONALLY SYMMETRIC REFLECTORS

Siniša Škokić, Enrica Martini, *Member, IEEE*, Stefano Maci, *Fellow, IEEE*

## ABSTRACT

It has been observed that the monostatic RCS of parabolic PEC reflectors vanishes at certain frequencies for broadside wave incidence. It has also been noticed that hyperbolic reflectors behave similarly, with very low RCS minima. This behaviour is explained by using Physical Optics (PO) and verified via a numerical full-wave analysis. Relations between the physical dimensions of the reflector and the characteristic values of the RCS (notch frequencies, minimum and maximum value), as well as a comparison of different canonical reflectors, are given. The interest in the phenomenon described is at present essentially speculative, since, as pointed out in the paper, there are some significant limitations which restrict its practical utilization.

## I. PRELIMINARY CONSIDERATIONS

In this paper, the wide-band monostatic RCS behaviour of rotationally symmetric reflectors illuminated from broadside direction is considered. The motivation for this particular analysis arises from noticing the occurrence of sharp minima in the monostatic RCS of some canonical reflectors.

In the case of axial incidence, the PO integral providing the field backscattered by a rotationally symmetric reflector can be interpreted as the radiation from an equivalent circular aperture with a particular current distribution, whereby the magnitude of the currents is constant and the phase depends on the reflector profile and on the frequency [1]. A reflector becomes electrically deeper with increasing frequency. Let us consider a reflector of monotone profile: when its depth becomes greater than  $\lambda/4$ , the field radiated from the inner part (the central disk on the equivalent aperture) will start to interfere destructively with the one radiated from the outer part (the outer ring), thus resulting in lower values of the scattered field and hence of the RCS. The maximum negative interference occurs when the reflector depth equals  $\lambda/2$ ; as the frequency increases further, a new constructively interacting area appears at the center of the aperture and the RCS increases again. Although this process has a periodic nature, it does not necessarily lead to a frequency-periodic RCS curve, since the level of interference between fields radiated from the different rings depends on the reflector profile.

It will be seen that the RCS minima equal 0 for the case of a parabolic reflector, revealing an interesting invisibility

Siniša Škokić is with the Department of Radiocommunications and Microwave Engineering, Faculty of Electrical Engineering and Computing, University of Zagreb, Croatia

Enrica Martini and Stefano Maci are with the Department of Information Engineering, University of Siena, Italy

phenomenon which, to the best of our knowledge, has not been previously detected. Although the scattering characteristics of an infinite parabolic reflector illuminated axially by a plane wave are well known [2], [3], only a few works have analysed the case of a finite paraboloid (see for instance [4], [5], [6]).

In the following, the broadside monostatic RCS of hyperbolic and parabolic reflectors are investigated; for the sake of comparison, the well-known results for the disk, the sphere and the cone are also briefly summarised.

## II. RCS OF A ROTATIONALLY SYMMETRIC PEC REFLECTOR

We start from the general case of a rotationally symmetric PEC reflector illuminated from broadside direction, with incident magnetic field defined as  $\vec{H}_i = H_0 e^{jkz} \hat{y}$ , as shown in Fig. 1. The origin of a cylindrical coordinate system is set at the apex of the reflector with the  $z$  axis being the axis of symmetry; the reflector radius is denoted with  $r$  and its depth with  $h$ . Since the reflector is rotationally symmetric,

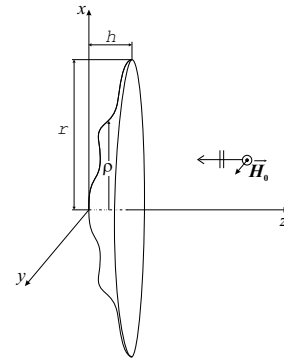


Fig. 1. Geometry for the reflector analyzed.

its equation is given as  $z = f(\rho)$ . Calculating the equivalent PO currents on the reflector surface as  $\vec{J}_{eq} = 2\hat{n} \times \vec{H}_i$  and bearing in mind that for monostatic broadside RCS only the  $x$ -component of the magnetic vector potential contributes to the scattered electric far-field, we obtain

$$\vec{E}_{sc} = (j\omega\mu H_0) \frac{e^{-jkR}}{R} \int_0^r e^{j2k f(\rho)} \rho d\rho \hat{x}. \quad (1)$$

The RCS  $\sigma$  is then calculated as

$$\sigma = \lim_{R \rightarrow \infty} 4\pi R^2 \frac{|\vec{E}_{sc}|^2}{|\vec{E}_i|^2}. \quad (2)$$

Denoting the integral in (1) with  $I$ , the RCS equation takes on the final simple form

$$\sigma = 4\pi k^2 |I|^2. \quad (3)$$

As can be seen from the previous formulas, the key point in obtaining the broadside monostatic RCS of a given reflector is the evaluation of the integral  $I$  in (3).

### III. CANONICAL SHAPES

The defining equation  $f(\rho)$  for different reflectors is reported in Table I, along with the corresponding values of  $I$  and  $\sigma$ . In the table,  $c = \cot(\theta/2)$ , where  $\theta$  is the cone nose angle,  $a$  and  $b$  are the semi-major and semi-minor axis of the hyperbola, and  $d_f$  is the focal length of the parabolic reflector.

#### A. Flat-Plate, Conical and Spherical Reflectors

The PO solutions for the RCS of flat-plate, conical and spherical reflectors, shown in Table I, are well-known. We nevertheless present them here to prepare the grounds for the discussion that follows. Their comparison is shown in Fig. 2.

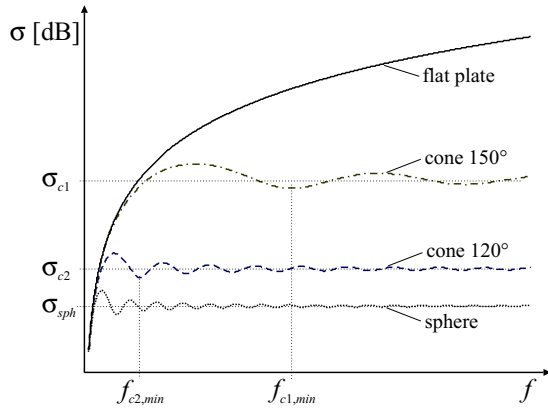


Fig. 2. Comparison of PO-calculated wideband monostatic RCS in broadside direction for a flat circular plate, a sphere, and two cones with different nose angles. All the reflectors have the same radius  $r$ .

We notice that the expressions for the RCS of the cone and the semi-sphere in Table I are basically the same. Indeed, for a  $90^\circ$ -cone the constant  $c$  equals 1 and the two solutions match exactly. On the other hand, in the limiting case when  $c \rightarrow 0$ , and for  $k \gg 1$ , the cone solution simplifies to the one of a flat-plate. Thus, one can consider the RCS of the flat-plate and the sphere as limiting cases of the RCS of cones (with nose angle greater than  $90^\circ$ ). Strictly speaking, the PO solution is not valid in the presence of a discontinuity such as the cone tip, but the solution is shown to agree reasonably well with the exact solution for the case of broadside monostatic RCS [1].

#### B. Hyperbolic Reflector

The RCS curve of a generic hyperbolic reflector is shown in Fig. 3 and compared with the corresponding curve of a parabolic reflector. One can notice that the first two terms in the expression of  $\sigma$  as reported in Table I tend to dominate over the last one with increasing frequency; the last term can be neglected for  $f \gg \frac{c_0}{2\pi h}$ ,  $c_0$  being the speed of light in free space. In this case, the expression simplifies to

$$\sigma_{hyp} = \frac{\pi b^4}{a^4} \left| ((a+h) - a e^{-j2kh}) \right|^2. \quad (4)$$

The minimum and the maximum RCS in the high-frequency region are given as

$$\begin{aligned} \sigma_{hyp}^{min} &= \frac{\pi b^4}{a^4} h^2 \\ \sigma_{hyp}^{max} &= \frac{\pi b^4}{a^4} (2a+h)^2, \end{aligned} \quad (5)$$

while the RCS minima occur for  $f = nc_0/2h$ , where  $n$  is a positive integer, that is, when the depth of the reflector equals  $n\lambda/2$ . Thus, the solution can be regarded as frequency-periodic, except in the low-frequency region, where the PO is not applicable anyway.

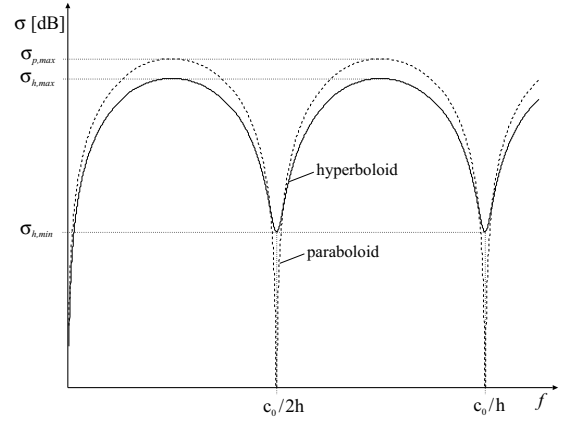


Fig. 3. Comparison of wideband broadside monostatic RCS for a generic parabolic and hyperbolic reflector having the same radius  $r$  and the same depth  $h$ , calculated with PO.

It is worth noting that, although not explicitly stated in the above equation, the maximum RCS value of a hyperbolic reflector of fixed radius  $r$  and depth  $h$  is independent of the parameters of its defining hyperbola. In other words, for any pair of values of the semi-major and semi-minor axis  $(a, b)$  which satisfy the condition that the reflector of radius  $r$  is deep  $h$ , the maximum RCS will have the same value, which equals  $\pi r^4/h^2$ . The minimum RCS value, on the other hand, does not exhibit such a property.

#### C. Parabolic Reflector

Bearing in mind that  $\frac{r^2}{4d_f}$  for a parabolic reflector actually denotes its depth  $h$  (Fig. 1), the solution from Table I simplifies to

$$\sigma_{par} = 16\pi d_f^2 \sin^2(kh). \quad (6)$$

The most interesting property that comes from (6) is the fact that the RCS completely vanishes at certain frequencies, as can be seen in Fig. 3. The equation also reveals that the maximum RCS of a parabolic reflector does not depend on its dimensions but merely on its focal length:

$$\sigma_{par}^{max} = 16\pi d_f^2 \quad (7)$$

and that also in this case the RCS minima occur for  $kh = n\pi$ , with  $n$  integer.

Furthermore, it is observed that in this case the RCS is strictly periodic with frequency. Although this is rigorously

TABLE I  
BROADSIDE MONOSTATIC RCS OF DIFFERENT CANONICAL SHAPES, CALCULATED WITH PO

reflector	sketch	$f(\rho)$	$I = \int_0^r e^{j2kf(\rho)} \rho d\rho$	$\sigma$
flat-plate	 $\leftarrow \parallel$	0	$\int_0^r \rho d\rho$	$\pi k^2 r^4$
cone	 $\leftarrow \parallel$	$-c\rho$	$\int_0^r e^{-j2kc\rho} \rho d\rho$	$\pi \left\{ \frac{1}{jc} \left[ \left( -r + \frac{j}{2kc} \right) e^{-j2kcr} - \frac{j}{2kc} \right] \right\}^2$
semi-sphere	 $\leftarrow \parallel$	$\sqrt{r^2 - \rho^2} - r$	$e^{-j2kr} \int_0^r e^{j2k\sqrt{r^2 - \rho^2}} \rho d\rho$	$\pi \left\{ \frac{1}{j} \left[ \left( -r + \frac{j}{2k} \right) e^{j2kr} - \frac{j}{2k} \right] \right\}^2$
hyperbola	 $\leftarrow \parallel$	$a\sqrt{1 + \frac{\rho^2}{b^2}} - a$	$e^{-j2ka} \int_0^r e^{j2ka\sqrt{1 + \frac{\rho^2}{b^2}}} \rho d\rho$	$\frac{\pi b^4}{a^4} \left  \left( (a+h) - a e^{-j2kh} - \frac{(1 - e^{-j2kh})}{j2k} \right) \right ^2$
parabola	 $\leftarrow \parallel$	$\frac{\rho^2}{4d_f}$	$\int_0^r e^{j2k\frac{\rho^2}{4d_f}} \rho d\rho$	$16\pi d_f^2 \sin^2 \left( \frac{kr^2}{4d_f} \right)$

true only for the parabolic reflector, an almost periodic behaviour is found for most of the reflectors analysed. This arises from the fact that for all reflectors the asymptotically dominant term is proportional to  $1 - e^{j2kh}$ ; as a consequence, for every frequency at which the reflector depth equals  $n\lambda/2$  there is a local minimum of RCS. The flatter the reflector, the farther apart the minima will be. This is best seen for the two cones discussed in the previous section, shown in Fig. 2.

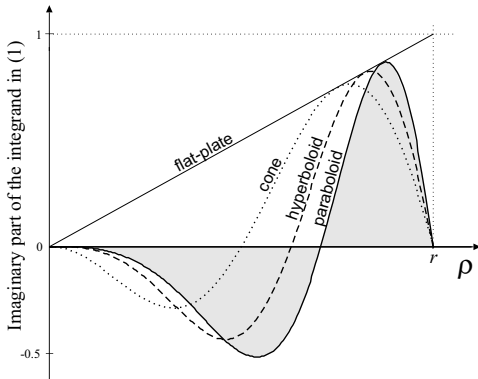


Fig. 4. The imaginary part of the integrand in (1), at  $f = c_0/2h$ : flat-plate reflector (thin line), parabolic reflector (thick line), hyperbolic reflector (dashed line) and conical reflector (dotted line). The shaded regions have the same area (parabolic reflector).

As anticipated in Sec. I, the minima in the RCS occur due to the interference between fields scattered from different parts (rings) of the reflector surface. This interaction can be understood better if one looks into the behaviour of the integrand in (1), whose imaginary part is shown in Fig. 4. The situation depicted there occurs at a "resonance" frequency, i.e. for  $f = c_0/2h$ , where there is a minimum of the RCS. It is seen that for the parabolic reflector (shaded) the inner and outer part contributions cancel each other out perfectly, while in the other reflectors cases one part dominates and the RCS has a non-zero value.

#### IV. AN INVISIBLE PARABOLA?

The most unexpected of the properties illustrated in previous sections is definitely the periodic vanishing of the RCS of a

parabolic reflector. One may think that this is brought about by the inaccuracy of the PO approximation. On the contrary, it is shown in this section that this phenomenon remains evident even when using a full-wave analysis.

#### A. Comparison between PO and MoM

A particular case of a parabolic reflector has been simulated by the Method of Moments (MoM) with a commercially available software (FEKO); the results have been compared with those provided by the PO analysis (Fig. 5) for a relatively small reflector ( $2r < \lambda$  at the lowest frequency). The two solutions match very well, confirming the validity of the PO approach. The difference between the curves is due mainly to the effect of creeping waves induced by the diffraction on the reflector edge, which is not taken into account in the PO analysis. It is worth noting, however, that the full-wave analysis predicts a very deep minimum at  $f = c_0/2h$ .

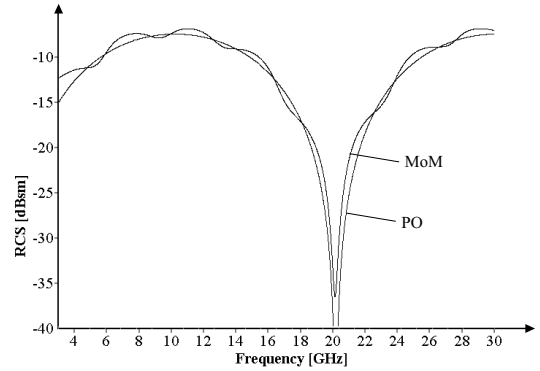


Fig. 5. Comparison of wideband broadside monostatic RCS for a parabolic reflector with  $r = 42.53$  mm,  $d_f = 60$  mm. The PO result agrees well with the MoM result even at the lowest frequency, where the reflector is less than one wavelength wide.

#### B. Paraxial Illumination

In order to investigate the spatial selectivity of the invisibility phenomenon described, we consider the case of a plane wave impinging on the reflector from an angle  $\theta$  with respect

to the  $z$ -axis (Fig. 1). We calculate the monostatic RCS again using the PO approximation. In this case, both the  $x$  and the  $z$  component of the equivalent currents have to be included for a rigorous analysis and the RCS can no longer be expressed in a simple form. Because of the oblique incidence, the integration in  $\phi$  gives rise to Bessel functions, which, in turn, can be represented via a Taylor expansion to yield a closed form solution.

The results obtained with this approach, shown in Fig. 6, were validated by comparison with those obtained via numerical integration and the ones provided by a MoM simulation. One sees that the value of the RCS at  $f = c_0/2h$  rapidly increases as the incidence direction moves away from the axis; this means that the phenomenon described in the previous Section exhibits a significant spatial selectivity, as one might have expected.

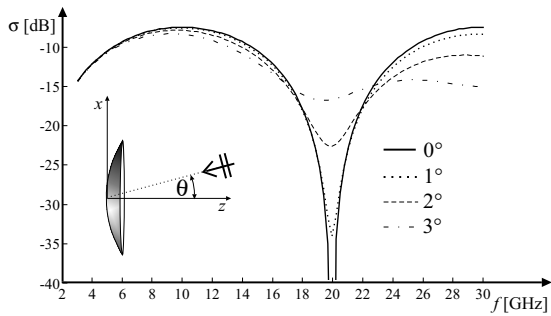


Fig. 6. Comparison of wideband broadside monostatic RCS of a parabolic reflector with  $r = 42.53$  mm,  $d_f = 60$  mm for different angles of incidence of the impinging plane wave.

### C. Effect of the Presence of Feeder

In most cases, a parabolic reflector is used in a reflector antenna system. In this case, the presence of a feeder at the reflector's focus may significantly perturbate the scattered field, this effect being most visible in the directions where the RCS has a null. In the results shown in Fig. 7, a mismatched feed located at the focus was represented by a flat metallic plate of the same dimensions. The results presented are obtained via a MoM analysis (FEKO). The RCS curve of the whole system no more shows the stealth behaviour. Moreover, with the increasing size of the feeder the RCS approaches that of the disk of the same radius. This is due to the fact that the reflected rays are focused on the feeder surface, then reflected back from the focus to the reflector at the same angle and re-reflected back in the broadside direction again as parallel rays. However, it is also worth noting that at the operating frequency of the antenna one can assume that the feeder is non-scattering, thus absorbing the singly reflected rays; this results in a significant decrease of the RCS level. (This phenomenon is however not accounted for in the simulated model.)

## V. CONCLUSION

The far field back scattering from some finite rotationally symmetric reflectors illuminated by a normally incident plane wave has been investigated. By applying the Physical Optics

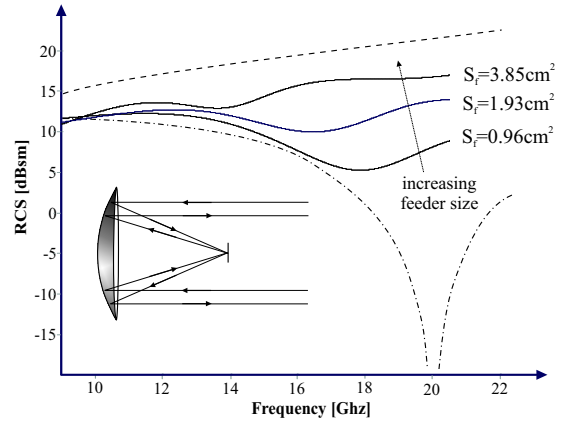


Fig. 7. Wideband broadside monostatic RCS for a parabolic reflector with  $r = 127.5$  mm,  $d_f = 540$  mm for different apertures of the feeder. The mismatched feeder is modelled as a flat rectangular PEC disk of aperture  $S_f$ . Results are compared to the RCS of a circular disk of the same radius (dashed line) and the parabolic reflector alone (dash-dotted line).

approximation, a closed form expression for the monostatic RCS has been obtained; in particular, it has been observed that this expression predicts the existence of deep minima at certain frequencies for some canonical reflectors. In particular, in the case of a paraboloid, the RCS vanishes at the frequencies where the reflector depth is an integer multiple of half-wavelength. This behaviour has been verified through a full wave analysis. It is finally observed that this invisibility phenomenon is hard to exploit in practice, since the value of the RCS increases rapidly with the angle of incidence of the illuminating plane wave and/or in presence of a mismatched feeder.

## REFERENCES

- [1] G. T. Ruck, D. E. Barrick, W. D. Stuart, and C. K. Krichbaum, *Radar Cross Section Handbook*, vol. 1, Plenum, New York, 1970.
- [2] C. E. Schensted, "Electromagnetic and acoustical scattering by a semi-infinite body of revolution," *J. Appl. Phys.*, vol. 26, pp. 306–308, 1955.
- [3] S. Roy and P. L. E. Uslenghi, "Exact scattering for axial incidence on an isorefractive paraboloid," *IEEE Trans. Antennas and Propagat.*, vol. 45, no. 10, pp. 1563, Oct. 1997.
- [4] G. Morris and T. S. M. Maclean, "On-axis fields of symmetric receiving paraboloid for normally incident wave," *IEEE Trans. Antennas and Propagat.*, vol. AP-25, no. 5, pp. 716–718, Sept. 1977.
- [5] M. S. Narasimhan, P. Ramanujam, and K. Raghavan, "GTD analysis of near-field and far-field patterns of a parabolic subreflector illuminated by a plane wave," *IEEE Trans. Antennas and Propagat.*, vol. AP-29, no. 4, pp. 654–660, July 1981.
- [6] J. E. Fletcher D. C. Jenn and A. Prata, "Radar cross section of symmetric parabolic reflectors with cavity-backed dipole feeds," *IEEE Trans. Antennas and Propagat.*, vol. 41, no. 7, pp. 992–994, July 1993.